



Seismic stability analysis of folded utility tunnel in loess stratum

Zongyuan Ma, Lei Liu*

Guizhou communications polytechnic, Guiyang, Guizhou, 551400, P. R. China

mzy_gogo@hotmail.com, *35781474@qq.com

Abstract. The finite element and time history analysis method was used to study the dynamic response of a single cabin and folded utility tunnel under seismic conditions, considering the effects of seismic intensity and peak acceleration. The dynamic response characteristics of the utility tunnel assembly connection, joint sealing, and utility tunnel wall were analyzed. The utility tunnel structure's regularity of displacement, stress, and response acceleration were obtained through three-dimensional finite element dynamic time history analysis. The result analysis found that the seismic acceleration response of the overall structure of the utility tunnel is lower than the dynamic response of the soil. The seismic intensity has the greatest impact on the seismic response of the utility tunnel structure, splicing joints, and connecting anchor bolts, and the input angle of the seismic wave has the lowest impact on the seismic stability of the folded utility tunnel.

Keywords: Underground folded utility tunnel; Earthquake; Dynamic response; Time history analysis; Numerical method.

1 Introduction

Urban underground comprehensive utility tunnel project has gradually become an important work of modern urban planning and development in China. The underground utility tunnel system can fundamentally solve the layout problem of Urban Pipelines, e.g., water supply and drainage, energy, and communication lines [1-3]. The threat of natural disasters to underground space projects has become prominent, e.g., earthquake disasters have the greatest impact on the safety and stability of underground space structures. At present, most large or medium-sized cities in Western China are in strong earthquake areas, and strong earthquakes will severely challenge the built urban underground space system [4]. Based on this background, this study starts from the dynamic behavior of loess, and process a series of research work on the dynamic stability and failure of urban underground utility tunnel system in loess area. The buried depth of most underground utility tunnels is relatively shallow (the average buried depth is 6m), and mostly installed in the form of integral prefabrication and assembly or cast-in-situ, and the cross-section is mostly rectangular or nearly rectangular. The dynamic response analysis on seismic response of utility tunnel under the seismic action are studied via

the large scale shaking table model test is frequently proceeded by researchers in recently years [5,6]. The dynamic response and vibration of the utility tunnel under seismic action also analyzed via numerical method by many researchers [7]. In this paper, the finite element and time history analysis method is used to calculate and analyze the dynamic response of a folded section and single warehouse underground utility tunnel in loess stratum under the seismic action. The nonlinear dynamic constitutive model of soil is adopted to analyze the interaction between the prefabricated sections of the underground utility tunnel and between the utility tunnel structure and soil under seismic load [8,9]. Through the three-dimensional finite element method, the time history of displacement, velocity, and acceleration, as well as the extreme results of stress and deformation of the utility tunnel structure are analyzed, and the seismic stability of the utility tunnel structure is analyzed. According to the characteristics of the underground utility tunnel structure, considering the interaction between soil and structure, this paper establishes a three-dimensional finite element model via the finite element code ABAQUS, and process the numerical simulation on the underground utility tunnel with folded section under earthquake conditions.

2 Engineering background

An underground utility tunnel project in the southern suburb of Xi'an city in Northwest China is used as an engineering case for analysis. The site of project is constructed by open excavation, C15 plain concrete cushion is laid when excavation is completed. The construction method proposed in this paper is to produce the standard section utility tunnel components and anchor bolt structure through the prefabricated utility tunnel production line. The prefabricated assembly utility tunnel has the advantages of high controllability of the production process, stable quality, good connection performance, high seismic resistance, good waterproof performance, simple construction, short construction period and so on. During construction, the standard section utility tunnel components shall be installed first, and then the variable path and elevation section of the pipeline shall be cast in situ. The utility tunnels are connected longitudinally and adjacent by prestressed anchor bolts. The strength grade of precast slab concrete is C40, the impermeability grade of concrete is P6, and all reinforcement grades are HRB400. The standard part of prefabricated box culvert is a tongue and groove structure, which is connected by prestressed reinforcement, and the tensioning force is not greater than 150kN. Cartesian rectangular coordinate system is used in the three-dimensional dynamic and static calculation and analysis, with the extension direction of the utility tunnel as the X axis, and the coordinate origin is selected at the center of the top of the utility tunnel; The buried depth direction of the utility tunnel is the y-axis, and the upward direction is the positive direction; The Z axis is perpendicular to the utility tunnel direction, and the vertical right is positive. The utility tunnel structure is a rectangular section, and the specific dimensions are shown in Fig. 1.

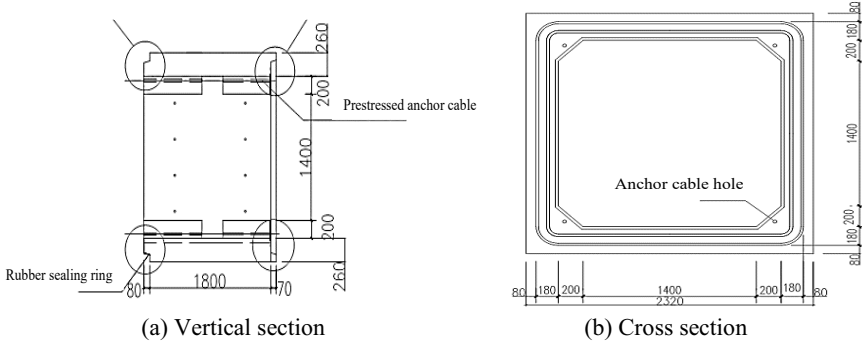


Fig. 1. cross section of prefabricated parts of utility tunnel

The acceleration time history of dynamic calculation input generates three kinds of artificial seismic acceleration amplitudes according to the design response spectrum curve recommended in code for seismic design of buildings (GB50011-2010) [4]. The ground motion peak acceleration 0.1g, 0.15g and 0.2g, respectively, and the standard design response spectrum given in the seismic code is shown in Fig. 2. The time history curves of seismic acceleration recommended by the three specifications are shown in Fig. 3. The three-dimensional dynamic finite element analysis of the utility tunnel project is carried out, and the dynamic response analysis of the utility tunnel when encountering the design peak ground acceleration earthquake during the operation period is mainly studied. The seismic acceleration amplitude input directions are horizontal and vertical respectively. Three-dimensional finite element method is used to analyze the time history of displacement, velocity, and acceleration of the utility tunnel structure, as well as the extreme results of stress and deformation.

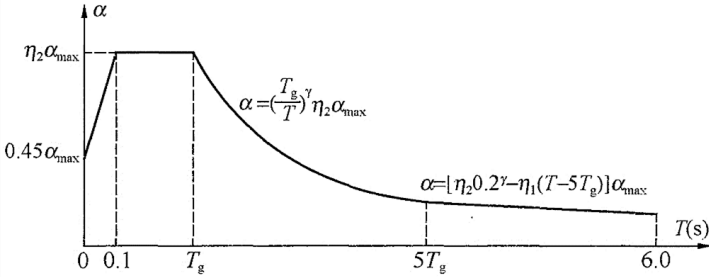


Fig. 2. standard design response spectrum

The attenuation index of the falling section of the curve shall be determined according to Eq. (1).

$$\gamma = 0.9 + \frac{0.05 - \zeta}{0.3 + 6\zeta} \tag{1}$$

The slope adjustment coefficient of the straight-line descent section shall be determined according to Eq. (2).

$$\eta_1 = 0.02 + \frac{0.05 - \zeta}{4 + 32\zeta} \quad (2)$$

Damping adjustment coefficient shall be determined according to Eq. (3).

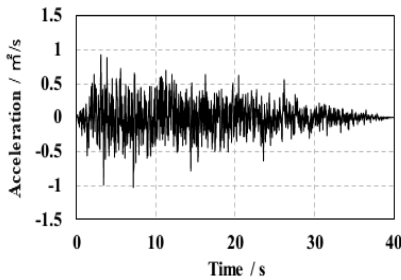
$$\eta_2 = 1 + \frac{0.05 - \zeta}{0.08 + 1.6\zeta} \quad (3)$$

Where, α is the earthquake influence coefficient, α_{\max} is the maximum value of the earthquake influence coefficient, t is the natural vibration period of the structure, T_g is the characteristic period, η_1 is the slope adjustment coefficient of the straight-line descent section, η_2 is the damping adjustment coefficient, γ is the attenuation index. The parameters are listed in the following table 1.

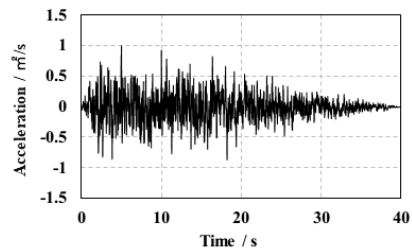
Table 1. Standard response spectrum for site bedrock design

Exceeding probability	α_{\max}	T_g	η_1	η_2	γ
50a 10%	2.5	0.40	0.0055	0.625	1.0

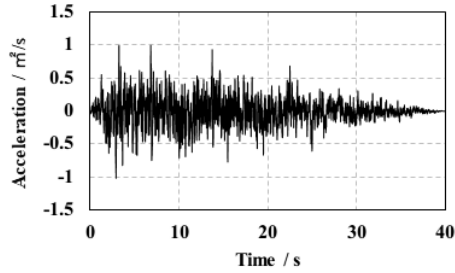
The horizontal and vertical seismic acceleration amplitudes are input to the bottom of the utility tunnel model along the x-axis (transverse), Y-axis (vertical) and z-axis (longitudinal), respectively, to calculate the stress and deformation analysis of the utility tunnel structure under seismic conditions. The calculation results of the working conditions of the pipe rack under the earthquake recommended by the code (peak acceleration of 0.1g, 0.2g, 0.3g) during the operation period are analyzed respectively. This paper mainly introduces the typical contours of the maximum value distribution of acceleration, stress and displacement of the pipe rack structure after the pipe rack is subjected to the earthquake with peak acceleration of 0.1g. From these maps, the variation law of the extreme value of stress and deformation in the key parts of the pipe rack during the earthquake process can be obtained. The so-called contour of the maximum value distribution of acceleration, stress and displacement refers to the drawing of the maximum value of acceleration, stress and displacement at each point in the whole process of the earthquake, and the time of occurrence of each point in the map is not consistent.



(a) Lengthways



(b) Vertical



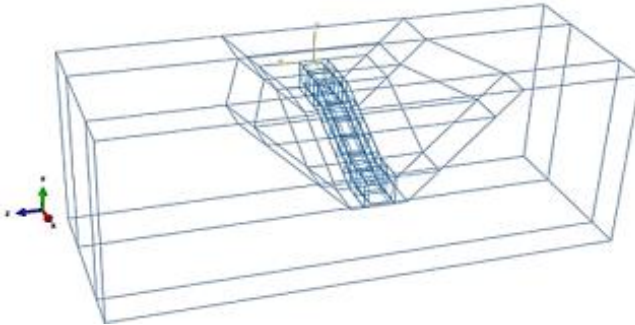
(c) Transverse

Fig. 3. Time history of seismic acceleration (Maximum acceleration 0.1g)

3 Numerical simulation

3.1 Finite element model

In this simulation calculation, two representative sections of the study area were intercepted, and the three-dimensional finite element calculation model of the straight utility tunnel without elevation change and the three-dimensional finite element calculation model of the curved utility tunnel with elevation change were used respectively, and the seismic responses of the two under the same conditions were compared. Take 8 prefabricated parts of the utility tunnel. The prefabricated parts of the utility tunnel are fixedly connected with prestressed anchor bolts. Cast in situ construction is adopted at the turn to improve the bearing capacity of the components. The anchor bolt is 1.5m long and its position is shown in Fig. 1. The three-dimensional model and FEM meshing of utility tunnel is shown in Fig. 4. The utility tunnel structure and soil are meshed into hexahedral eight node solid element and anchor bolt structure beam element.



(a) Folded utility tunnel simulation area

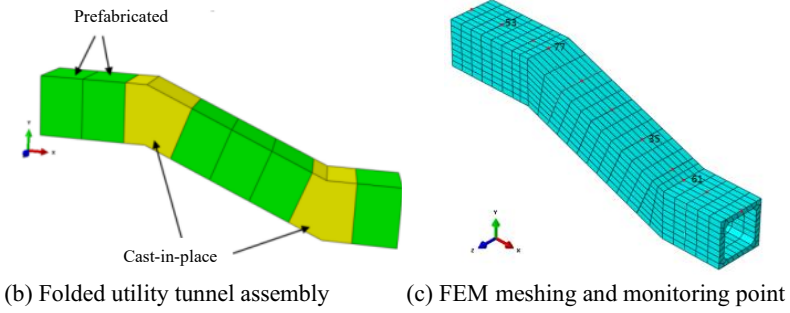


Fig. 4. Three-dimensional model of utility tunnel

3.2 Boundary condition setting and mechanical material parameters

During dynamic calculation, viscoelastic damping boundary is adopted around the model to prevent seismic acceleration amplitudes from reflecting at the boundary. The three components of seismic acceleration time history are applied at the bottom of the model, and the vertical design peak acceleration is taken as 2/3 of the horizontal direction. The calculation grid is the same as the static calculation condition. Before the dynamic time history analysis of the utility tunnel, the self weight in-situ stress field balance calculation is carried out. After the in-situ stress field balance is carried out under the action of gravity field, the seismic accelerations in the X, y and Z directions are loaded, and the dynamic calculation and analysis of the utility tunnel are carried out under the action of gravity. The first-order modal shapes of the utility tunnel are shown in Fig. 5, and the natural frequencies of the straight-line and folded utility tunnel models are 2.9Hz.

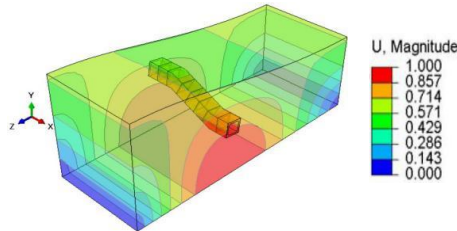


Fig. 5. First order modal shape of utility tunnel

A dynamic visco-elasto-plastic constituted model for soil is established in this study to analyze the seismic slope stability problem. The visco-elasto-plastic behavior is predicted by the Kelvin cell in series with a plastic cell corresponds to the Mohr-Coulomb criterion. The visco-elastic stress-strain relation is as follows:

$$\sigma_{ij} = 2G\epsilon_{ij} + \lambda\epsilon_v\delta_{ij} + 2\eta_G\dot{\epsilon}_{ij} + \eta_\lambda\dot{\epsilon}_v \quad (4)$$

where K and G are the bulk and shear modulus, η_K and η_G are the dynamic viscosity for volume and shear deformation. The values of η_K and η_G are determined by the following formula (Clough 1975)

$$\eta_G = \frac{2GD}{2\pi f}, \quad \eta_k = \frac{2KD}{2\pi f} \quad (5)$$

where D is the damping ratio, f is the frequency of the structure. The following function for the relationship of the shear modulus reduction versus cyclic shear strain was suggested by Hardin and Drnevich (Hardin and Drnevich 1972),

$$G/G_{\max} = 1/(1 + \gamma/\gamma_{\text{ref}}) \quad (6)$$

$$D/D_{\max} = (\gamma/\gamma_{\text{ref}})/(1 + \gamma/\gamma_{\text{ref}}) \quad (7)$$

where γ_{ref} is reference shear strain, and the shear modulus and damping ratio reduction factor G/G_{\max} and D/D_{\max} are 0.5 when $\gamma = \gamma_{\text{ref}}$. Fig. 6 shows the relationship of the shear modulus reduction versus equivalent shear strain in % for sand (Seed 1986), clay (Sun 1988), and silty loess (this study) compared with the theoretical prediction of the Hardin's function [9]. The mechanical behavior of soil would be linear elastoplasticity (no dynamic characteristics of soil will be taken into account) if the reference shear strain $\gamma_{\text{ref}} \rightarrow \infty$ and the damping ratio $D = 0$. The shear modulus of the soil will be decreased rapidly if the value of γ_{ref} is small. The dynamic parameters of the soil for seismic slope stability analysis in this study are as follows: the reference shear strain $\gamma_{\text{ref}} = 0.1$, and the maximum damping ratio $D_{\max} = 0.2$. The main materials involved in the calculation are loess stratum, concrete material of utility tunnel, connecting anchor bolt, etc. The determination of calculation parameters is mainly based on the values provided by the entrusting party. Among them, the linear constitutive relationship of the material utility tunnel concrete material is calculated according to the concrete damage, and the concrete calculation parameters refer to the test of C30 concrete standard sample uniaxial compressive strength test [8,9]. The parameters and values required for loess dynamic calculation are shown in Table 2.

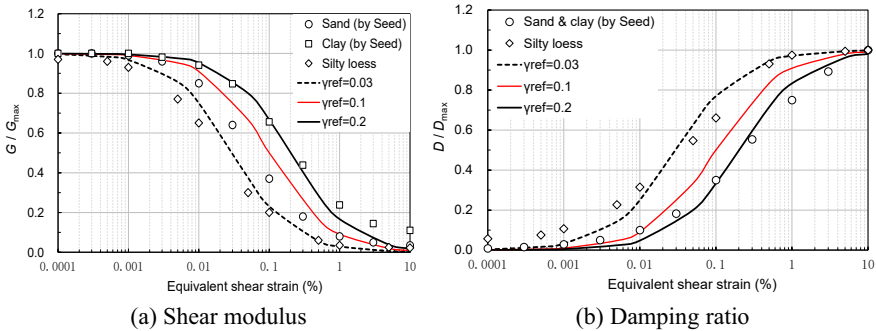


Fig. 6. Relationship of shear modulus and damping ratio versus equivalent shear strain (in %) for soil and comparison with the theoretical prediction of Hardin's function

Table 2. Values of dynamic calculation parameters for loess

Density ρ (kg/m^3)	G_{\max} (MPa)	Poisson's ratio ν	γ_{ref}	D_{\max}	c (kPa)	ϕ ($^\circ$)
1800	40	0.25	0.1	0.2	30	20.0

4 Results ad analysis

4.1 Seismic response of pipe rack structure

The calculation results show that during the seismic process of the curved utility tunnel, the maximum horizontal displacement of the utility tunnel in the X direction is 3.15cm, and the maximum vertical deformation displacement is 18.36cm, which is mainly concentrated in the buried depth change section of the utility tunnel near the shallow buried place, and the maximum horizontal displacement in the Z direction is 4.2cm, which is mainly concentrated in the buried depth change section of the utility tunnel near the deep buried place near the bottom plate of the utility tunnel. The maximum vertical acceleration of the utility tunnel is 0.93m/s^2 , which is mainly concentrated in the middle buried depth of the variable buried section of the utility tunnel. The maximum horizontal acceleration in the X direction is 0.18m/s^2 , which is mainly concentrated in the buried depth change section of the utility tunnel near the shallow buried place; The maximum Z-direction acceleration is 0.21m/s^2 , which is mainly in the middle of the two side plates in the buried depth change section of the utility tunnel. Compared with the curved utility tunnel, the maximum displacement and maximum acceleration of the straight utility tunnel are increased, and the calculated results are shown in Fig. 7. Fig. 8 and 9 shows the comparison of maximum deformation and displacement time history of soil mass and utility tunnel structure under different seismic intensities.

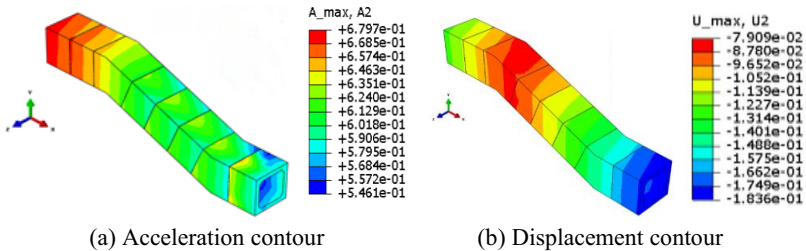


Fig. 7. Comparison of maximum value of vertical seismic response of utility tunnel

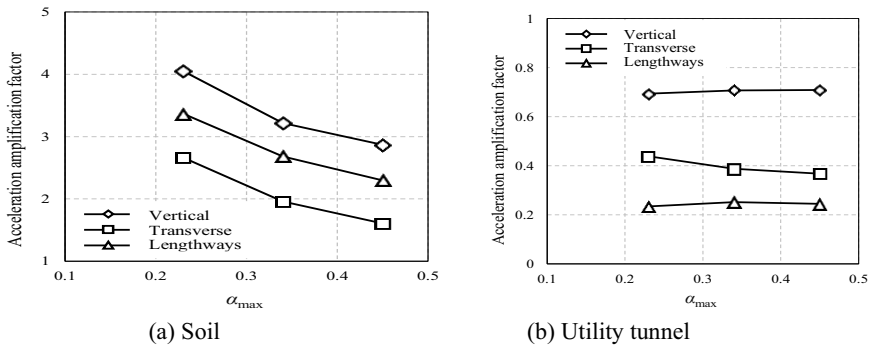


Fig. 8. Acceleration amplification of soil and utility tunnel structure during earthquake

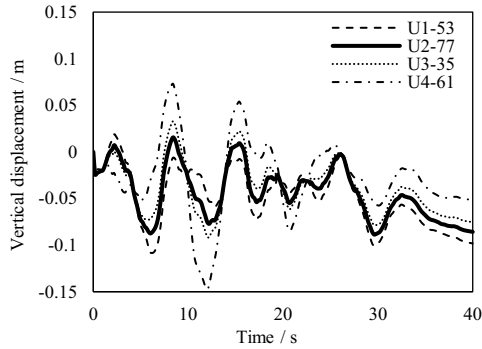


Fig. 9. Vertical displacement time history of monitoring point at the top of utility tunnel

4.2 Influence of input angle for seismic acceleration amplitude

The seismic response corresponding to the comprehensive utility tunnel and soil mass is analyzed when the peak acceleration is 0.2g. Only the input direction of the horizontal seismic acceleration amplitude component is changed, and the input angle is the included angle between the horizontal seismic acceleration amplitude component. The seismic response of soil and utility tunnel structure under different seismic acceleration amplitude input angles is shown in Fig. 10. It can be seen from the seismic response of the utility tunnel at different incident angles that the incident angles of each component of the seismic acceleration amplitude have a certain impact on the response acceleration of the soil, and the dynamic response of the soil in the direction of the seismic acceleration amplitude input angle along and perpendicular to the utility tunnel (90 °) is the largest. The input angle has little effect on the utility tunnel structure.

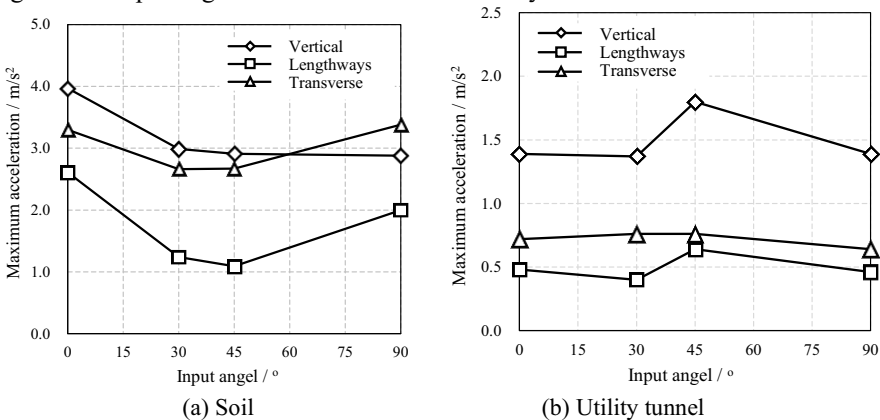


Fig. 10. Relationship between seismic acceleration input angle and Reaction acceleration

4.3 Seismic response of utility tunnel joint

During the seismic process of the curved utility tunnel, the maximum stress and strain of the prefabricated utility tunnel joint: the maximum opening displacement is 0.098cm, the maximum horizontal shear stress is 0.79MPa, the maximum vertical shear stress is 0.48MPa, the maximum horizontal slip displacement is 1.61cm, and the maximum vertical slip displacement is 1.15cm. As shown in Fig. 11. The analysis of the tension displacement and maximum slip value of the spliced joint under different peak accelerations of the utility tunnel is shown in Fig. 12. From the settlement results of joint deformation, the joint tension deformation during and after the earthquake is very small, and the joint deformation is mainly transverse and vertical slip deformation, in which the transverse horizontal slip deformation is the largest, and the deformation after the earthquake is greater than that during the earthquake.

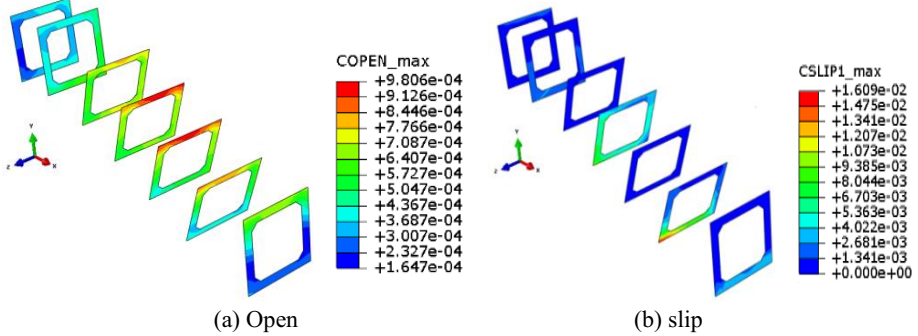
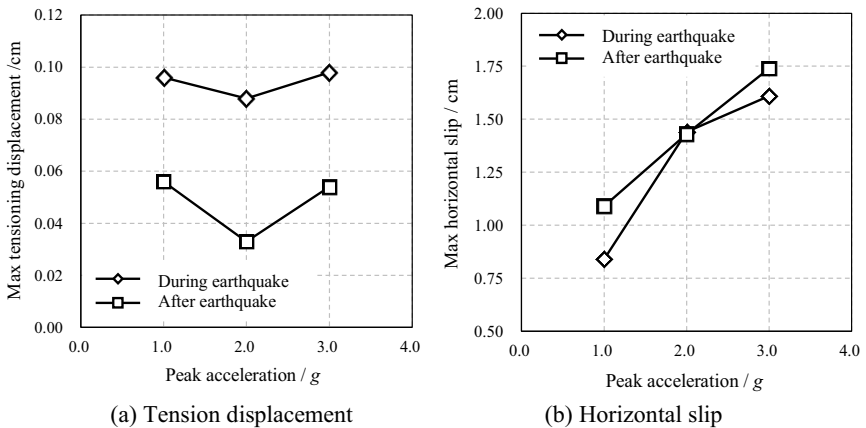
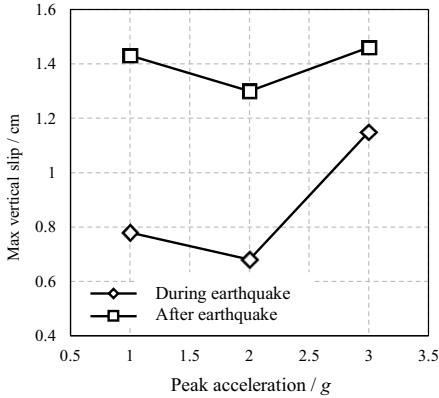
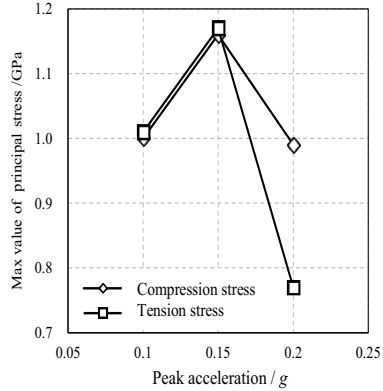


Fig. 11. Maximum displacement contour of utility tunnel's splicing joint (unit: m)





(c) Vertical slip

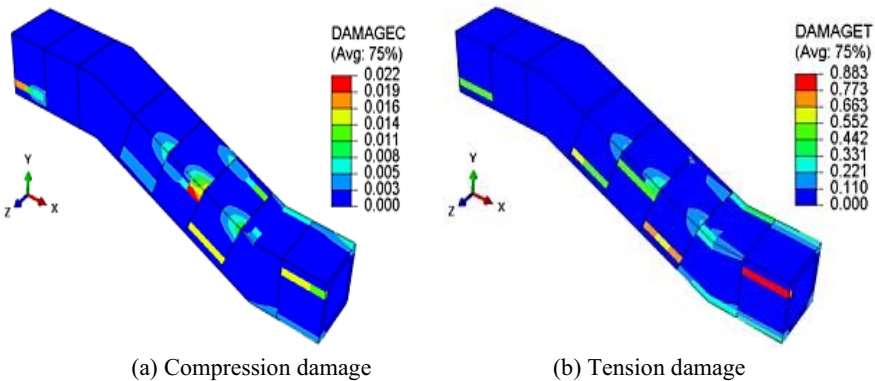


(d) Maximum tensile stress of anchor cable

Fig. 12. Deformation of splicing seams and anchor cable's stress under different peak accelerations of earthquake

4.4 Stress and structural damage of anchor bolt of utility tunnel

Through the finite element simulation of this section of utility tunnel, it is found that the tensile deformation of anchor bolt is mainly concentrated in the buried depth of the utility tunnel during the earthquake process [10]. The maximum value of the small principal stress and the maximum value of the large principal stress of the anchor bolt do not exceed the yield stress of the anchor bolt under the action of earthquake, the stress deformation of anchor bolt of straight utility tunnel is smaller than that of folded utility tunnel. To facilitate comparison and analysis, the damage of concrete under seismic action of folded utility tunnel and straight utility tunnel under peak acceleration of 0.1g is selected for analysis, and the calculation results yielded by the finite element code ABAQUS are shown in Fig. 13.



(a) Compression damage

(b) Tension damage

Fig. 13. Distribution of damage area of utility tunnel structure after earthquake

5 Conclusion

In this paper, the finite element and time history analysis method is used to study the dynamic response of the single tank utility tunnel under earthquake conditions, mainly studying the dynamic response characteristics of the utility tunnel assembly joint, joint water-tight seal, and utility tunnel wall under earthquakes with different intensities, peak accelerations, and incident directions. Through the three-dimensional finite element dynamic time history analysis, the basic regularity of displacement, velocity, acceleration, stress, and deformation of the utility tunnel structure are obtained, and the seismic stability of the overall structure of the utility tunnel is analyzed. The main conclusions are as follows:

(1) The seismic response of the utility tunnel structure, especially the acceleration response, is lower than the dynamic response of the soil, indicating that the utility tunnel structure buried in the soil is restrained by the surrounding rock, which significantly reduces the impact of seismic action.

(2) Among the three influencing factors of seismic intensity, seismic peak acceleration and seismic input angle, the seismic intensity has the greatest impact on the seismic response of utility tunnel structure, splicing joints and connecting anchor bolts, followed by the seismic peak acceleration, and the impact of seismic acceleration amplitude input angle is the least. It shows that seismic energy and destructive force are the key factors affecting the stability of the wall structure, splicing and connection structure of the underground utility tunnel. The seismic resistance can be enhanced efficiently by strengthen the splicing and connection between the sections of the utility tunnel.

(3) This study can be further extended to the analysis of site characteristics (e.g., site response spectrum characteristics, soil properties, and other geological conditions) and the influence of multi compartment utility tunnel structure.

Acknowledgment

The research described in this paper was funded by the Guizhou Science & Technology Cooperation Platform Talent (No. CXTD[2021]008), and the major scientific and technological research project of Guizhou transportation department (No. 2023-122-001).

References

1. People's Republic of China Ministry of housing and urban rural development. Technical code for urban comprehensive utility tunnels project (GB50838-2015), Beijing: China Planning Press, 2015. https://www.mohurd.gov.cn/gongkai/zhengce/zhengcfilelib/201505/20150526_224135.html.
2. Genger K T, Hammad A, Oum N. Multi-objective optimization for selecting potential locations of multi-purpose utility tunnels considering agency and social lifecycle costs. *Tunneling and Underground Space Technology*, 2023, 140: 105305. <https://doi.org/10.1016/j.tust.2023.105305>.

3. Alaghbandrad A, Hammad A. Framework for multi-purpose utility tunnel lifecycle cost assessment and cost-sharing. *Tunnelling and Underground Space Technology*, 2020, 104: 103528. <https://doi.org/10.1016/j.tust.2020.103528>.
4. National Standard Building Seismic Design Code Management Group, Building Seismic Design Code (GB50011-2010, Revised in 2016), Beijing: China Construction Industry Press, 2016. https://www.mhurd.gov.cn/gongkai/fdzdgknr/zqyj/202112/20211231_763760.html?eqid=d928b27f000537d50000000364571717.
5. Darli CM, Tang A, Huang D, Zhang J. Large scale shaking table model test and analysis on seismic response of utility tunnel in nonhomogeneous soil. *Earthquake Engineering and Engineering Vibration*. 2021;20(2):505-515. <https://doi.org/10.1007/s11803-021-2035-6>.
6. Li, Z; Luo, QY and Zhou, R. Experimental research on seismic response of split-type pre-fabricated utility tunnels through shaking table tests. *Earthquake Engineering & Structural Dynamics*, 2022, 51 (12): 2880-2903. <https://doi.org/10.1002/eqe.3706>.
7. Huang D L, Zong Z L, Tang A P, Huang Z Y, Liu Q. Dynamic response and vibration isolation of pipes inside a utility tunnel passing through nonhomogeneous soil under seismic action. *Soil Dynamics and Earthquake Engineering*, 2022, 163: 107522. <https://doi.org/10.1016/j.soildyn.2022.107522>.
8. Ma Z Y, Dang F N, Liao H J. Numerical study of the dynamic compaction of gravel soil ground using the discrete element method. *Granular Matter*, 2014, 16(6): 881-889. <https://link.springer.com/article/10.1007/s10035-014-0529-x>.
9. Ma Z Y, Liao H J, Dang F N, Cheng Y X. Seismic slope stability and failure process analysis using explicit finite element method. *Bulletin of Engineering Geology and the Environment*, 2021, 80:1287-1301. <https://link.springer.com/article/10.1007/s10064-020-01989-3>.
10. Valdenebro J V, Gimena F N, López J J. Construction process for the implementation of urban utility tunnels in historic centres. *Tunnelling and Underground Space Technology*, 2019, 89: 38-49. <https://doi.org/10.1016/j.tust.2019.03.026>.

Open Access This chapter is licensed under the terms of the Creative Commons Attribution-NonCommercial 4.0 International License (<http://creativecommons.org/licenses/by-nc/4.0/>), which permits any noncommercial use, sharing, adaptation, distribution and reproduction in any medium or format, as long as you give appropriate credit to the original author(s) and the source, provide a link to the Creative Commons license and indicate if changes were made.

The images or other third party material in this chapter are included in the chapter's Creative Commons license, unless indicated otherwise in a credit line to the material. If material is not included in the chapter's Creative Commons license and your intended use is not permitted by statutory regulation or exceeds the permitted use, you will need to obtain permission directly from the copyright holder.

